

Deep inelastic scattering with a tagged photon: QED corrections for the Σ method

H. Anlauf^{a,b}

Fachbereich Physik, Siegen University, D-57068 Siegen, Germany

Received: 12 January 1999 / Published online: 22 March 1999

Abstract. After a brief review of the kinematics of deep inelastic scattering (DIS) within the so-called Σ method, we derive the necessary formulae for the treatment of QED radiative corrections to DIS originating from hard photon radiation. The results are applied to a calculation of the corrections to DIS with a tagged photon with next-to-leading logarithmic accuracy under HERA conditions. It turns out that the next-to-leading logarithmic corrections are quite important for the Σ method. We also discuss the dependence of the corrections on the longitudinal structure function of the proton, F_L , in the region of low Q^2 and moderate x .

1 Introduction

The determination of the structure functions of the proton, $F_2(x, Q^2)$ and $F_L(x, Q^2)$, over a broad range of the kinematic variables belongs to the most important tasks of the H1 and ZEUS experiments at the HERA ep collider. Especially the extension of these measurements to the range of small Bjorken $x < 10^{-4}$ and Q^2 of a few GeV^2 is of particular interest, as it provides a testing ground for our attempts to understand the details of the dynamics of quarks and gluons inside the nucleon.

Whilst the structure function F_2 can be extracted quite easily from the experimental data, it is more difficult to determine the longitudinal structure function F_L . A direct method that relies only on measured data requires running the collider at different center-of-mass energies. However, besides impairing the high-energy program of the machine, running at reduced beam energies also increases some systematic errors, (e.g., luminosity uncertainties), in the experimental analysis.

These problems are circumvented by employing a method suggested by Krasny et al. [1] that utilizes radiative events. This method takes advantage of a photon detector (PD) in the very forward direction, as seen from the incoming lepton (electron or positron) beam. Such a device is part of the luminosity monitoring system of both the H1 and ZEUS experiments.

The idea of this method is that emission of photons in a direction close to the incoming lepton corresponds to a reduction of the effective beam energy. This effective beam energy for each radiative event is determined from the energy of the hard photon observed (tagged) in the

PD. Early analyses that make use of these radiative events for a determination of F_2 were already published in [2,3]. No QED radiative corrections were taken into account in these analyses. The feasibility of a determination of F_L was studied in [4].

Recently, the H1 collaboration presented preliminary results of a refined analysis with newer data [5]. In this analysis, the authors chose different methods of determination of the kinematic variables¹ (the e -method, where the kinematic variables are obtained from a measurement of the scattered lepton, and the Σ method) in different (x, Q^2) bins in order to reduce the experimental systematic error. However, since the calculations of the QED radiative corrections to DIS with a tagged photon [7–9] did not cover the Σ method, the corrections were only applied to part of the data in [5]. It is the purpose of the present work to extend these analytical calculations to the Σ method.

The Σ method, as proposed by Bassler and Bernardi [10], tries to combine the momenta of the outgoing lepton and hadrons judiciously in order to reduce experimental systematic uncertainties on the determination of the kinematic variables especially in the kinematic region of low Q^2 where other methods are limited by e.g., detector resolution or energy calibration.

With the help of the quantity²

$$\Sigma_h \equiv \sum_h (E_h + p_{z,h}), \quad (1)$$

¹ For a discussion of the most common methods to determine kinematic variables and further references, see e.g. [6]

² Note that in this paper we take the positive z -axis along the initial lepton direction, unlike [10] who chose the direction of the incoming proton beam

^a Supported by Bundesministerium für Bildung, Wissenschaft, Forschung und Technologie (BMBF), Germany

^b e-mail: anlauf@hep.tu-darmstadt.de

where the sum runs over the detected hadrons, and E_h and $p_{z,h}$ are the energy and z -component of the respective particle, the kinematic variables x_Σ , y_Σ and Q_Σ^2 are defined via

$$\begin{aligned} y_\Sigma &= \frac{\Sigma_h}{\Sigma_h + E'_e(1 + \cos\theta)}, & Q_\Sigma^2 &= \frac{E_e'^2 \sin^2\theta}{1 - y_\Sigma}, \\ x_\Sigma &= \frac{Q_\Sigma^2}{y_\Sigma S}. \end{aligned} \quad (2)$$

Here $S = 4E_e E_p$, where E_e and E_p are the beam energies of the lepton and proton beam, respectively, and E'_e and θ are the energy and scattering angle of the outgoing lepton, measured with respect to the direction of the initial lepton.

One of the known advantages of the Σ method is its insensitivity of the determination of y_Σ and Q_Σ^2 to undetected emission of a hard photon collinear to the incoming lepton (initial state radiation, ISR).

The Σ method has already been used in several analyses of the H1 collaboration. However, the author is not aware of any publications on an analytical (i.e., non-Monte Carlo) treatment of QED radiative corrections to deep inelastic scattering (DIS) using the Σ kinematic variables³ beyond the collinear (leading log) approximation [12, 13]. The presumable reason is that the Σ method has only been introduced long after the start of data taking at HERA. Therefore, this paper starts with a brief introduction to the kinematics of radiative DIS in the Σ method. Section 3 extends the considerations to the case of DIS with an exclusive tagged photon, but specialized to the conditions at HERA, and provides the relevant formulae to calculate the radiative corrections to the tagged photon cross section, based on the results of [9]. Some results for HERA experimental conditions are presented in Sect. 4, and Sect. 5 contains our conclusions. Finally, the appendices collect several technical details.

2 Kinematics in the Σ method

This section is devoted to a basic review of the Σ method. Here we shall prepare an appropriate framework for the treatment of radiative corrections to radiative deep inelastic scattering,

$$e(p) + P(P) \rightarrow e(p') + X(P') + \gamma(k), \quad (3)$$

i.e., DIS with single hard photon emission. The extension to the process with an additional tagged photon in the

³ As the tagged photon cross section represents a radiative correction to the DIS cross section [7], one can in principle calculate the QED corrections to the former for any choice of kinematic variables with the help of a Monte Carlo event generator for DIS that properly implements the necessary higher order QED corrections to DIS. However, no generator exists for the calculation of QED corrections beyond leading logarithms, and the leading log generator KRONOS [11] uses approximations for photon emission in the very forward direction that make it useless for the present task

forward direction is straightforward and will be performed in the next section.

Let us begin by stating our conventions for the kinematics in the HERA lab frame that are used throughout this paper. We shall take the orientation of the coordinate frame such that the positive z -axis points in the direction of the incoming lepton beam, and the momentum of the scattered lepton lies in the x - z -plane:

$$\begin{aligned} P &= (E_p, 0, 0, -p_p), \\ p &= (E_e, 0, 0, p_e), \\ p' &= (E'_e, p'_e \sin\theta, 0, p'_e \cos\theta), \\ k &= E_\gamma(1, \sin\vartheta \cos\varphi, \sin\vartheta \sin\varphi, \cos\vartheta). \end{aligned} \quad (4)$$

As the beam energies E_p, E_e , as well as the energy of the scattered lepton, E'_e , are always large compared to the proton mass, M , and the electron mass, m , we shall take $p_p = E_p$, $p_e = E_e$, and $p'_e = E'_e$, wherever possible.

Since we assume $E_p \gg M$, we may replace the definition of the variable Σ_h in (1) by

$$\Sigma_h := \frac{P \cdot (P' - P)}{E_p}. \quad (5)$$

This allows us to similarly reexpress the definitions (2) of the kinematic variables x_Σ , y_Σ , and Q_Σ^2 through scalar products of four-momenta via

$$y_\Sigma = \frac{P \cdot (P' - P)}{P \cdot (P' - P + p')}, \quad (6)$$

$$Q_\Sigma^2(1 - y_\Sigma) = \frac{4(p \cdot p')(P \cdot p')}{S}, \quad (7)$$

$$x_\Sigma = \frac{Q_\Sigma^2}{y_\Sigma S}, \quad (8)$$

where

$$S = 2P \cdot p.$$

One important thing to note here is the nonlinear dependence of the kinematic variables y_Σ and Q_Σ^2 on the energy and scattering angle of the outgoing lepton, while it is linear in the electron-only method (e -method).

As we are dealing with the kinematics of a process with real photon emission, it is convenient to define an invariant quantity κ , that represents the energy of the outgoing photon in units of the energy of the incoming lepton, as measured in the rest frame of the incoming proton,

$$\kappa := \frac{P \cdot k}{P \cdot p}. \quad (9)$$

Energy and momentum conservation of the process (3) obviously requires $0 \leq \kappa < 1$. In the special case of emission of the photon collinear to the incoming lepton, κ also represents the energy fraction of the initial lepton taken by the photon in the HERA lab frame.

Using momentum conservation (3) and relations (6) and (9), it is easy to see that

$$P \cdot (P' - P) = (1 - \kappa)y_\Sigma P \cdot p = (1 - \kappa)y_\Sigma \cdot \frac{1}{2}S. \quad (10)$$

To proceed, let us express the remaining scalar products of external momenta in terms of invariant kinematic variables and other measured quantities. We find

$$\begin{aligned} P \cdot p' &= \frac{1 - y_\Sigma}{y_\Sigma} P \cdot (P' - P) = (1 - \kappa)(1 - y_\Sigma) \cdot \frac{1}{2} S, \\ p \cdot p' &= \frac{x_\Sigma y_\Sigma^2 S^2}{4P \cdot (P' - P)} = \frac{x_\Sigma y_\Sigma}{1 - \kappa} \cdot \frac{1}{2} S. \end{aligned} \quad (11)$$

Furthermore, from the photon's energy $E_\gamma =: x_\gamma E_e$ and angles ϑ and ϑ' with respect to the incoming and final lepton, respectively, we obtain

$$\begin{aligned} p \cdot k &= x_\gamma E_e^2 (1 - \cos \vartheta), \\ p' \cdot k &= x_\gamma E_e E_e' (1 - \cos \vartheta'), \end{aligned} \quad (12)$$

where the angle ϑ' is calculated from (4),

$$\cos \vartheta' = \cos \theta \cos \vartheta + \sin \theta \sin \vartheta \cos \varphi. \quad (13)$$

Next, we rewrite the left-hand sides of the relations (11) in the HERA lab frame as

$$\begin{aligned} P \cdot p' &= E_p E_e' (1 + \cos \theta), \\ p \cdot p' &= E_e E_e' (1 - \cos \theta), \end{aligned} \quad (14)$$

to derive explicit expressions for the energy and scattering angle of the outgoing lepton in the HERA frame,

$$\begin{aligned} E_e' &= (1 - \kappa)(1 - y_\Sigma) E_e + \frac{x_\Sigma y_\Sigma}{1 - \kappa} E_p, \\ \cos \theta &= \frac{(1 - \kappa)^2 (1 - y_\Sigma) E_e - x_\Sigma y_\Sigma E_p}{(1 - \kappa)^2 (1 - y_\Sigma) E_e + x_\Sigma y_\Sigma E_p}, \end{aligned} \quad (15)$$

that may further be used to eliminate E_e' in the second equation of (12), or to trade the azimuthal angle φ in favor of the angle ϑ' .

It is now straightforward to obtain the expressions for the momentum transfer to the hadronic system

$$\begin{aligned} Q_h^2 &\equiv -(P - P')^2 = -(p - p' - k)^2 \\ &= \frac{x_\Sigma y_\Sigma S}{1 - \kappa} + 2k \cdot (p - p'), \end{aligned} \quad (16)$$

the hadronic scaling variable

$$x_h \equiv \frac{Q_h^2}{2P \cdot (p - p' - k)} = \frac{Q_h^2}{(1 - \kappa) y_\Sigma S}, \quad (17)$$

and the invariant mass of the hadronic system,

$$\begin{aligned} W^2 &= (P')^2 = (P + p - p' - k)^2 \\ &= M^2 + y_\Sigma \left[1 - \kappa - \frac{x_\Sigma}{(1 - \kappa)} \right] S - 2k \cdot (p - p') \\ &= M^2 + \frac{1 - x_h}{x_h} Q_h^2. \end{aligned} \quad (18)$$

In the last equation we explicitly retained the proton mass.

The kinematic limit for the phase space of the radiated photon may be derived by requiring that the invariant

mass of the hadronic system be larger than the threshold for pion production,

$$W^2 \geq \bar{M}^2, \quad \text{where } \bar{M} = M + m_\pi. \quad (19)$$

The actual upper limit on the photon energy as a function of the emission angle, $E_\gamma^{\max} = E_\gamma^{\max}(\theta; \vartheta, \varphi) = E_\gamma^{\max}(\theta; \vartheta, \vartheta')$ is obtained in general by solving a quadratic or cubic equation; for details see appendices A and B.

Before we conclude this section, we shall give the relations between the kinematic variables in the Σ method and in the e -only method. From the scalar products (11), we find:

$$\begin{aligned} 1 - y_e &= (1 - \kappa)(1 - y_\Sigma) \implies y_e = y_\Sigma + \kappa(1 - y_\Sigma), \\ x_e y_e &= \frac{x_\Sigma y_\Sigma}{1 - \kappa} \implies x_e = \frac{x_\Sigma y_\Sigma}{(1 - y_\Sigma)[y_\Sigma + \kappa(1 - y_\Sigma)]}. \end{aligned} \quad (20)$$

The Jacobian between these two sets is

$$\begin{aligned} \mathcal{J} &\equiv \det \left(\frac{\partial(x_e, y_e)}{\partial(x_\Sigma, y_\Sigma)} \right) = \frac{y_\Sigma}{y_\Sigma + \kappa(1 - y_\Sigma)} \\ &= \frac{y_\Sigma}{y_e}. \end{aligned} \quad (21)$$

The reader may easily verify that the above formulae are consistent with the collinear limits discussed in [12].

3 DIS with a tagged photon

After having discussed the kinematics in the Σ method, let us now turn to our primary aim, the description of radiative corrections to neutral current deep inelastic scattering with an exclusive tagged photon for the HERA collider.

3.1 Kinematics and lowest order cross section

As already explained in the introduction and described in more detail in [1] (and references cited therein), the experimental detection of photons emitted in the very forward direction is actually possible at the HERA collider due to the presence of photon detectors (PD) that are part of the luminosity monitoring systems of the H1 and ZEUS experiments. These PD's cover an angular range very close to the direction of the incoming lepton beam, ($\vartheta_\gamma \equiv \angle(\mathbf{p}, \mathbf{k}) \leq \vartheta_0 \approx 5 \cdot 10^{-4}$ rad).

Thus, the process under consideration corresponds to the reaction

$$e(p) + p(P) \rightarrow e(p') + \gamma(k) + X(P') + [\gamma(k_2)], \quad (22)$$

where $\gamma(k)$ denotes the collinearly emitted, exclusively measured (tagged) photon, and $[\gamma(k_2)]$ indicates an additional (i.e., second) photon in the case of the radiative correction to the lowest order process.

A set of kinematic variables that is adapted to take into account tagged collinear radiation is given by the *shifted*

Bjorken variables [1, 7, 9].⁴ Expressed in terms of the measured quantities, Σ_h (see 5), the energy E'_e and angle θ of the scattered lepton, and the energy of the tagged photon, they read

$$\hat{y} = \frac{\Sigma_h}{\Sigma_h + E'_e(1 + \cos\theta)}, \quad \hat{Q}^2 = \frac{E_e'^2 \sin^2\theta}{1 - \hat{y}},$$

$$\hat{x} = \frac{\hat{Q}^2}{\hat{y}zS}. \quad (23)$$

Here we denoted by z the energy fraction of the lepton after initial state radiation of a collinear photon,

$$z = \frac{2P \cdot (p - k)}{S} = \frac{E_e - E_\gamma}{E_e}, \quad (24)$$

where E_γ represents the energy deposited in the forward PD.

The above definition (23) corresponds to (6)–(8), but with an effectively reduced center-of-mass energy, zS . It is obvious that in the case of the Σ method only \hat{x} is affected by collinear initial state radiation, as was already found in [10].

In analogy to the case of ordinary DIS, we may rewrite the kinematic variables in a Lorentz invariant fashion:

$$\hat{y} = \frac{P \cdot (P' - P)}{P \cdot (P' - P + p')}, \quad \hat{Q}^2 = \frac{4(zp \cdot p')(P \cdot p')}{(1 - \hat{y})zS},$$

$$\hat{x} = \frac{\hat{Q}^2}{\hat{y}zS}. \quad (25)$$

The Born cross section, integrated over the solid angle of the photon detector ($0 \leq \vartheta_\gamma \leq \vartheta_0$, $\vartheta_0 \ll \theta$) takes a factorized form (see also [1, 14, 7, 9]):

$$\frac{1}{\hat{y}} \frac{d^3\sigma_{\text{Born}}}{d\hat{x}d\hat{y}dz} = \frac{\alpha}{2\pi} P(z, L_0) \tilde{\Sigma}, \quad (26)$$

where

$$\begin{aligned} \tilde{\Sigma} &\equiv \tilde{\Sigma}(\hat{x}, \hat{y}, \hat{Q}^2) \\ &= \frac{2\pi\alpha^2(-\hat{Q}^2)}{\hat{Q}^2\hat{x}\hat{y}^2} \left[2(1 - \hat{y}) - 2\hat{x}^2\hat{y}^2 \frac{M^2}{\hat{Q}^2} \right. \\ &\quad \left. + \left(1 + 4\hat{x}^2 \frac{M^2}{\hat{Q}^2} \right) \frac{\hat{y}^2}{1 + R} \right] F_2(\hat{x}, \hat{Q}^2), \end{aligned}$$

with

$$P(z, L_0) = \frac{1 + z^2}{1 - z} L_0 - \frac{2z}{1 - z}, \quad L_0 = \ln \left(\frac{E_e^2 \vartheta_0^2}{m^2} \right),$$

$$\hat{Q}^2 = \hat{x}\hat{y}zS, \quad \alpha(-\hat{Q}^2) = \frac{\alpha}{1 - \Pi(-\hat{Q}^2)}, \quad (27)$$

$$R = R(\hat{x}, \hat{Q}^2) = \left(1 + 4\hat{x}^2 \frac{M^2}{\hat{Q}^2} \right) \frac{F_2(\hat{x}, \hat{Q}^2)}{2\hat{x}F_1(\hat{x}, \hat{Q}^2)} - 1.$$

⁴ Here we shall use the notation \hat{x} etc. of [9] to avoid confusion between shifted Bjorken variables and the usual ones. Although \hat{x} etc. are determined in the Σ method, we drop the index Σ in order to not overload the notation

The quantities F_2 and F_1 denote the proton structure functions. Note that we explicitly include the correction from vacuum polarization $\Pi(-\hat{Q}^2)$ in the virtual photon propagator, and that we neglect the contributions from Z-boson exchange and γ -Z interference, because we are interested mostly in the kinematic region of small momentum transfer \hat{Q}^2 .

The cross section (26) describes the process (22) to lowest order in perturbation theory. The radiative corrections to this cross section are composed of contributions by corrections due to virtual photon exchange, soft photon emission, and emission of a second hard photon, with one of the hard photons being tagged in the PD. Because of its coarse granularity, we shall assume that the PD cannot measure photons individually but only their total energy when two hard photons simultaneously hit the PD in different locations.

3.2 Virtual and soft corrections

The virtual and soft corrections to the lowest order cross section are simply obtained from the calculation for a measurement using the e -method by substitution. For the sake of completeness, we quote the result from [9]:

$$\frac{1}{\hat{y}} \frac{d^3\sigma_{\text{V+S}}}{d\hat{x}d\hat{y}dz} = \frac{\alpha^2}{4\pi^2} [P(z, L_0)\tilde{\rho} - T] \tilde{\Sigma}, \quad (28)$$

with

$$\begin{aligned} \tilde{\rho} &= 2(L_Q - 1) \ln \frac{\Delta^2}{Y} + 3L_Q + 3 \ln z - \ln^2 Y \\ &\quad - \frac{\pi^2}{3} - \frac{9}{2} + 2\text{Li}_2 \left(\frac{1+c}{2} \right), \\ T &= \frac{1+z^2}{1-z} (A \ln z + B) - \frac{4z}{1-z} L_Q \ln z \\ &\quad - \frac{2 - (1-z)^2}{2(1-z)} L_0 + \mathcal{O}(\text{const}), \\ A &= -L_0^2 + 2L_0 L_Q - 2L_0 \ln(1-z), \\ B &= [\ln^2 z - 2\text{Li}_2(1-z)] L_0, \\ L_Q &= \ln \frac{\hat{Q}^2}{zm^2}, \\ \text{Li}_2(t) &= - \int_0^t \frac{du}{u} \ln(1-u). \end{aligned} \quad (29)$$

Here Δ denotes the infrared cutoff for the emission of a soft photon in addition to the hard one, $\Delta = E_{\gamma_2}^{\text{max}}/E_e$. Furthermore,

$$Y \equiv \frac{E'_e}{E_e} = z(1 - \hat{y}) + \hat{x}\hat{y} \frac{E_p}{E_e} \quad \text{and}$$

$$c \equiv \cos\theta = \frac{z(1 - \hat{y})E_e - \hat{x}\hat{y}E_p}{z(1 - \hat{y})E_e + \hat{x}\hat{y}E_p} \quad (30)$$

follow from the formulae of the previous section with the replacement $p \rightarrow zp$, as the energy loss due to the tagged

collinear photon is known and already taken into account in the determination of the kinematic variables.

It should be noted that in (28)–(29) and also further below we retain only terms with double or single large logarithms of the small electron mass m , i.e., terms of order $\alpha^2 L^2$ and $\alpha^2 L$, with L being one of L_0 or L_Q . As the lowest order cross section (26) is of order αL relative to the DIS cross section, we shall denote the terms of order $\alpha^2 L^2$ as leading (LL) and those of order $\alpha^2 L$ as next-to-leading logarithmic (NLL) ones.

3.3 Double hard bremsstrahlung

Besides the soft and virtual corrections to the lowest order process, we have to consider also the corrections from hard bremsstrahlung, which in the present case corresponds to double hard bremsstrahlung.

In the calculation of the contributions from the emission of two hard photons, it is convenient to decompose the phase space into same three regions discussed in [9]: *i*) both hard photons hit the forward photon detector, i.e., both are emitted within a narrow cone around the lepton beam ($\vartheta_{1,2} \leq \vartheta_0$, $\vartheta_0 \ll 1$); *ii*) one photon is tagged in the PD, while the other is collinear to the outgoing lepton ($\vartheta'_2 \equiv \angle(\mathbf{k}_2, \mathbf{p}') \leq \vartheta'_0$); and finally *iii*) the second photon is emitted at large angles (i.e., outside the defined narrow cones) with respect to both incoming and outgoing lepton momenta. The last kinematic domain is denoted as the semi-collinear one. For the sake of simplicity, we shall always assume below that $\vartheta'_0 \ll 1$.

The contribution from the kinematic region *i*) (both hard photons being tagged, and only the sum of their energies measured), has the form [9]:

$$\begin{aligned} \frac{1}{\hat{y}} \frac{d^3 \sigma_i^{\gamma\gamma}}{d\hat{x} d\hat{y} dz} &= \frac{\alpha^2}{8\pi^2} L_0 \left[L_0 \left(P_{\Theta}^{(2)}(z) \right. \right. \\ &+ 2 \frac{1+z^2}{1-z} \left(\ln z - \frac{3}{2} - 2 \ln \Delta \right) \Big) \\ &+ 6(1-z) + \left(\frac{4}{1-z} - 1 - z \right) \ln^2 z \\ &\left. - 4 \frac{(1+z)^2}{1-z} \ln \frac{1-z}{\Delta} \right] \tilde{\Sigma} \\ &+ \mathcal{O}(\text{const}), \end{aligned} \quad (31)$$

with

$$\begin{aligned} P_{\Theta}^{(2)}(z) &= 2 \left[\frac{1+z^2}{1-z} \left(2 \ln(1-z) - \ln z + \frac{3}{2} \right) \right. \\ &\left. + \frac{1}{2} (1+z) \ln z - 1 + z \right]. \end{aligned}$$

The contributions to the kinematic regions *ii*) and *iii*) in the present case are slightly more complicated than for the purely leptonic measurement described in [9]. Before discussing the contributions to the cross section from radiation almost collinear to the final state lepton, we shall

therefore extend our treatment of the kinematics now and exhibit the necessary changes to the notation introduced in Sect. 2.

To this end, let us recall the introduction (9) of the variable κ . Again we define

$$\kappa := \frac{P \cdot k_2}{P \cdot p} = x_2 \frac{1 + \cos \vartheta}{2}. \quad (32)$$

Here x_2 is the energy of the second (i.e., non-collinear) photon that is not tagged in the PD, in units of the initial lepton energy, and ϑ is its emission angle with respect to the incoming lepton. By similar reasoning as in the previous section, one can easily see that we presently have $0 \leq \kappa < z$.

On the other hand, the tagging of the collinear hard photon with energy E_γ in the PD corresponds to a reduction of the effective initial lepton energy by a factor of z (see 24). The corresponding relations between measured quantities and invariant variables are simply obtained from (10)–(18) via the simultaneous substitutions $E_e \rightarrow zE_e$, $S \rightarrow zS$, $\kappa \rightarrow \kappa/z$. Therefore, e.g., (15) now read

$$\begin{aligned} E'_e &= (z - \kappa)(1 - \hat{y})E_e + \frac{\hat{x}\hat{y}z}{z - \kappa} E_p, \\ \cos \theta &= \frac{(z - \kappa)^2(1 - \hat{y})E_e - \hat{x}\hat{y}zE_p}{(z - \kappa)^2(1 - \hat{y})E_e + \hat{x}\hat{y}zE_p}. \end{aligned} \quad (33)$$

In addition we define

$$\begin{aligned} \hat{Q}_t^2 &\equiv 2zp \cdot p' = \frac{z\hat{Q}^2}{z - \kappa} = \frac{\hat{x}\hat{y}z^2 S}{z - \kappa}, \\ \hat{t} &\equiv -2zp \cdot k_2 = 2x_2 z E_e^2 (1 - \cos \vartheta), \\ \hat{s} &\equiv 2p' \cdot k_2 = 2x_2 E_e E'_e (1 - \cos \vartheta'). \end{aligned}$$

The momentum transfer to the hadronic system and the true hadronic scaling variable are

$$\begin{aligned} Q_h^2 &= -(zp - p' - k_2)^2 = \hat{Q}_t^2 - \hat{t} - \hat{s}, \\ x_h &= \frac{Q_h^2}{2P \cdot (zp - p' - k_2)} = \frac{Q_h^2}{(z - \kappa)\hat{y}S}. \end{aligned} \quad (34)$$

The kinematic limit $x_2^{\max}(\vartheta, \vartheta')$ for the emission of the second hard photon is again obtained by requiring that the hadronic mass

$$W^2 = (P + zp - p' - k_2)^2 = M^2 + \frac{1 - x_h}{x_h} Q_h^2 \quad (35)$$

be larger than the inelastic threshold, \bar{M}^2 . More details can be found in appendix B.

The contribution to the radiative cross section from the semi-collinear region *iii*) is obtained from the corresponding expression in the case of the e -method (see eqs. 3.7f of [9]),

$$\begin{aligned} \frac{1}{\hat{y}} \frac{d^3 \sigma_{iii}^{\gamma\gamma}}{d\hat{x} d\hat{y} dz} &= \frac{\alpha^2}{\pi^2} P(z, L_0) \\ &\times \int \frac{d^3 k_2}{|\mathbf{k}_2|} \frac{\alpha^2(Q_h^2)}{Q_h^4} I^\gamma(zp, p', k_2), \end{aligned} \quad (36)$$

with

$$\begin{aligned} \Gamma &= -\frac{1}{\hat{s}\hat{t}} \left\{ GF_1(x_h, Q_h^2) \right. \\ &\quad + \left[x_h [z^2 + (z - \kappa)^2(1 - \hat{y})^2] S^2 - \frac{x_h M^2}{Q_h^2} G \right. \\ &\quad \left. \left. + [(z - \kappa)(1 - \hat{y})(\hat{Q}_l^2 - \hat{s}) - z(\hat{Q}_l^2 - \hat{t})] S \right] \right. \\ &\quad \left. \times F_2(x_h, Q_h^2) \right\}, \\ G &= Q_h^4 - 2\hat{s}\hat{t} + \hat{Q}_l^4, \end{aligned} \quad (37)$$

and \hat{s} , \hat{t} , \hat{Q}_l^2 , Q_h^2 , and x_h as defined above. The angular part of the k_2 -integration is clearly restricted to the kinematic region *iii*), i.e., the full solid angle with the exception of the separately treated cones around the incoming and outgoing lepton.

Let us finally turn to the discussion of the kinematic region *ii*). As was already discussed in [9], we expect that the contribution of this region to the observed cross section will depend on the experimental event selection, i.e., on the method of measurement of the scattered particles. We shall focus on the very same two possibilities. The first one is denoted as an *exclusive* (or bare) event selection, as only the scattered lepton is measured; the hard photon that is emitted almost collinearly (i.e., within a small cone with opening angle $2\vartheta'_0$ around the momentum of the outgoing lepton) remains undetected or is not taken into account in the determination of the kinematic variables. The second, more realistic case (from an experimental point of view) is a *calorimetric* event selection, when only the sum of the energies of the outgoing lepton and photon is actually measured if the photon momentum lies inside a small cone with opening angle $2\vartheta'_0$ along the direction of the final lepton.

First, in the case of an exclusive event selection, when only the scattered lepton is detected, we obtain for $\vartheta'_0 \ll 1$ (similarly to 3.3 of [9])⁵

$$\begin{aligned} \frac{1}{\hat{y}} \frac{d^3\sigma_{ii,\text{excl}}^{\gamma\gamma}}{d\hat{x} d\hat{y} dz} &= \frac{\alpha^2}{4\pi^2} P(z, L_0) \\ &\quad \times \int_{\zeta_0}^{\zeta_{\max}} \frac{d\zeta}{\zeta^2} \left[\frac{1 + \zeta^2}{1 - \zeta} (\tilde{L} - 1) + (1 - \zeta) \right] \tilde{\Sigma}_f, \\ \tilde{\Sigma}_f &\equiv \tilde{\Sigma}(x_f, y_f, Q_f^2), \end{aligned} \quad (38)$$

where

$$\begin{aligned} \tilde{L} &= L'_0 + 2 \ln \frac{Y(\zeta)}{Y(1)}, \quad L'_0 \equiv \ln \frac{E_e^2 \vartheta_0'^2}{m^2} + 2 \ln Y(1), \\ Y(\zeta) &= \frac{\zeta^2 z(1 - \hat{y}) + [1 - \hat{y}(1 - \zeta)]^2 \hat{x}\hat{y}\varepsilon}{\zeta [1 - \hat{y}(1 - \zeta)]} \end{aligned}$$

⁵ We have of course kept the small but finite electron mass in the kinematic region of collinear radiation wherever necessary. See e.g. [15] for a very readable presentation

$$\begin{aligned} x_f &= \frac{[1 - \hat{y}(1 - \zeta)]^2}{\zeta^3} \hat{x}, \quad y_f = \frac{\zeta \hat{y}}{1 - \hat{y}(1 - \zeta)}, \\ Q_f^2 &= \frac{1 - \hat{y}(1 - \zeta)}{\zeta^2} \hat{Q}^2, \quad \varepsilon = \frac{E_p}{E_e}, \\ \zeta_{\max} &= 1 - \frac{\Delta}{Y(1)} = 1 - \frac{\Delta}{z(1 - \hat{y}) + \hat{x}\hat{y}\varepsilon}, \end{aligned} \quad (39)$$

and ζ_0 is the real solution in the interval $(0, 1)$ of the cubic equation

$$\zeta_0^3 - \hat{x} [1 - \hat{y}(1 - \zeta_0)]^2 - \frac{\bar{\Delta}_m}{\hat{y}z} [1 - \hat{y}(1 - \zeta_0)] \zeta_0^2 = 0, \quad (40)$$

with $\bar{\Delta}_m = (\bar{M}^2 - M^2) / S$, see also appendix B. We note in passing that the form of the leading logarithmic piece of (38) agrees with the corresponding terms of the calculation performed in [12].

Last, in the case of a calorimetric event selection, where only the sum of the energies of the outgoing lepton and photon is measured if the photon momentum lies inside the small cone with opening angle $2\vartheta'_0$ along the direction of the final lepton, the corresponding contribution reads

$$\begin{aligned} \frac{1}{\hat{y}} \frac{d^3\sigma_{ii,\text{cal}}^{\gamma\gamma}}{d\hat{x} d\hat{y} dz} &= \frac{\alpha^2}{4\pi^2} P(z, L_0) \\ &\quad \times \int_0^{\zeta_{\max}} d\zeta \left[\frac{1 + \zeta^2}{1 - \zeta} (L'_0 - 1 + 2 \ln \zeta) + (1 - \zeta) \right] \tilde{\Sigma} \\ &= \frac{\alpha^2}{4\pi^2} P(z, L_0) \left[(L'_0 - 1) \left(2 \ln \frac{Y(1)}{\Delta} - \frac{3}{2} \right) \right. \\ &\quad \left. + 3 - \frac{2\pi^2}{3} \right] \tilde{\Sigma}. \end{aligned} \quad (41)$$

The total contribution from QED radiative corrections is finally found by adding up (28), (31), (36), and, depending on the chosen event selection, (38) or (41). The reader may easily verify that the unphysical IR regularization parameter Δ cancels in the sum, as it should.

It is important to note that the angle ϑ'_0 plays only the rôle of an intermediate regulator for the bare event selection and drops out in the final result. In the calorimetric case there are no large logarithmic contributions from final state radiation as long as ϑ'_0 does not become too small, since the mass singularity that is connected with the emission of the photon off the scattered lepton is canceled in accordance with the Kinoshita-Lee-Nauenberg theorem [16]. For more details we refer the reader to [9].

4 Numerical results

In order to illustrate our results, we shall now present some numerical values obtained for the leading and next-to-leading radiative corrections. To facilitate the comparisons of the results for the Σ method with those for determinations of the kinematic variables based on a lepton-only measurement [7, 9], we used as input

$$E_e = 27.5 \text{ GeV}, \quad E_p = 820 \text{ GeV}, \quad \vartheta_0 = 0.5 \text{ mrad}. \quad (42)$$

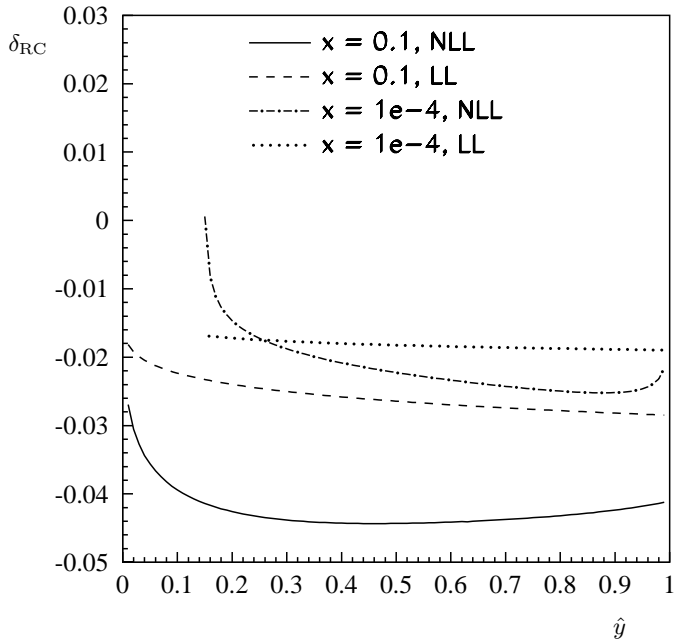


Fig. 1. Radiative corrections δ_{RC} (43) with leading and next-to-leading logarithmic accuracy at $\hat{x} = 0.1$ and $\hat{x} = 10^{-4}$ and a tagged photon energy of 5 GeV. No cuts have been applied to the phase space of the second (semi-collinear) photon

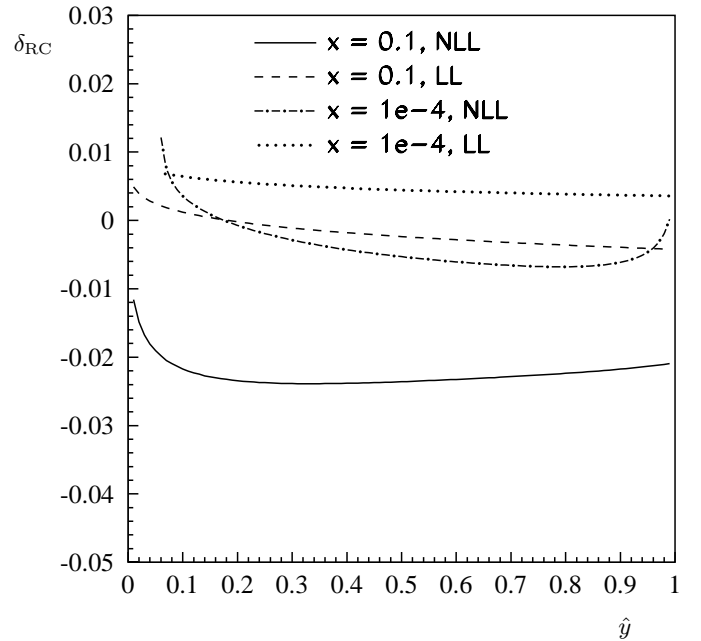


Fig. 2. Radiative corrections δ_{RC} (43) with leading and next-to-leading logarithmic accuracy at $\hat{x} = 0.1$ and $\hat{x} = 10^{-4}$ and a tagged photon energy of 20 GeV. No cuts have been applied to the phase space of the semi-collinear photon

Unless stated otherwise, we chose the ALLM97 parameterization [17] as structure function with $R = 0$, no cuts were applied to the photon phase space, and we assumed a calorimetric event selection. For the sake of simplicity we took a fixed representative angular resolution of $\vartheta'_0 = 50$ mrad for the electromagnetic calorimeter to separate nearby hits by an electron or positron and a hard photon, which is close to realistic for the H1 detector at HERA. Also we disregard any effects due to the magnetic field bending the scattered charged lepton away from a collinear photon.

Figure 1 compares the radiative correction

$$\delta_{\text{RC}} = \frac{d^3\sigma}{d^3\sigma_{\text{Born}}} - 1 \quad (43)$$

with leading and next-to-leading logarithmic accuracy at $\hat{x} = 0.1$ and $\hat{x} = 10^{-4}$ and for a tagged energy of $E_{\text{PD}} = 5$ GeV. The corresponding results for a tagged energy of $E_{\text{PD}} = 20$ GeV are shown in Fig. 2. The apparent cutoff at small \hat{y} for small \hat{x} is due to touching of the narrow cones defined by the solid angle covered by the photon detector and the cone around the final state lepton.

At first sight the radiative corrections, being only of the order of a few percent, look rather small as compared to, e.g., a leptonic measurement. However, this apparent suppression of the leading logarithmic part of the QED radiative corrections is easily traced back to the known weak dependence on initial state radiation of the determination of the kinematic variables (23)–(25) using the Σ method [10,6]. On the other hand, the pure next-to-

leading logarithmic corrections are unsuppressed, as this “cancellation mechanism” does not work for non-collinear photon radiation.

When we choose a bare event selection instead of a calorimetric one, the radiative corrections do become slightly larger. This is demonstrated in Fig. 3 that compares the radiative corrections for both selection schemes. The difference between the curves may be easily understood by noticing that in the calorimetric case the contribution from final state corrections to the cross section is proportional to the relatively small logarithm $\ln \vartheta'_0$, while it depends on the larger logarithm $\ln E'_e/m$ in the bare case.

Next we shall study the influence of a photon energy cut on the radiative corrections. For simplicity, we assume an emission angle independent cut $E_{\gamma 2}^{\text{max}}$, which may be realized at large angles by rejecting events that show energy in the electromagnetic calorimeter sufficiently separated from the final state lepton, and for small angles by a cut on the variable

$$\delta := \Sigma_h + E'_e(1 + \cos \theta) - 2(E_e - E_{\text{PD}}),$$

which is about twice the energy of a photon that is lost outside the PD. Figures 4 and 5 illustrate the dependence of the radiative corrections on an energy cut on the semi-collinear (lost) photon. The influence of a rather loose cut of $E_{\gamma 2} < 5$ GeV is significant, especially at the larger value of $\hat{x} = 0.1$, although the inclusive corrections were seen to be quite small.

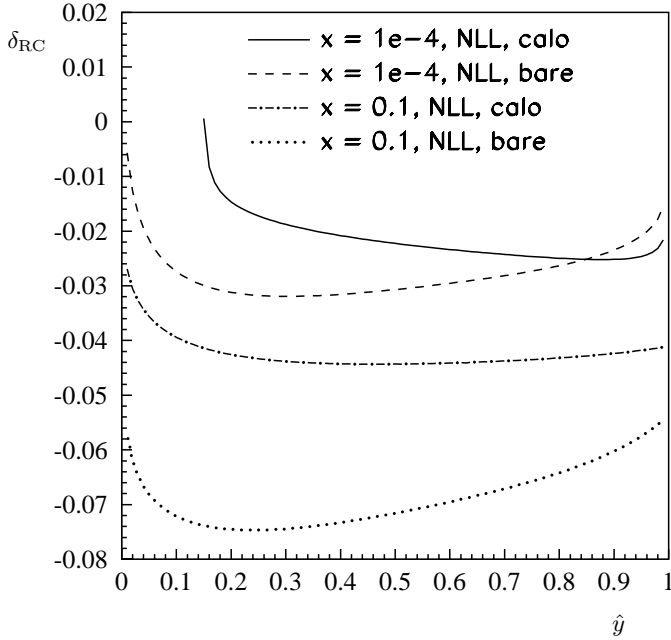


Fig. 3. Comparison of the radiative corrections for calorimetric (“calo”) vs. bare measurement of the scattered lepton at $\hat{x} = 10^{-4}$ and at $\hat{x} = 0.1$ for a tagged photon energy of 5 GeV

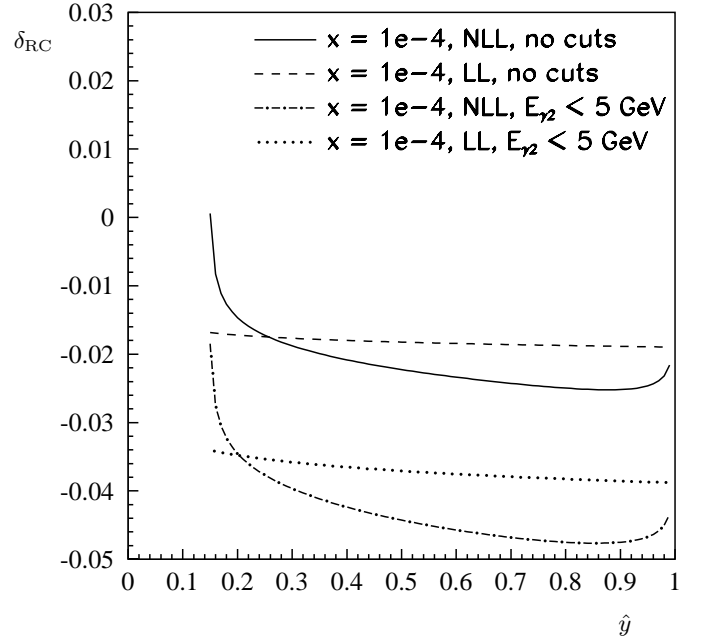


Fig. 5. Comparison of the cut dependence of the radiative corrections at $\hat{x} = 10^{-4}$ for a tagged photon energy of 5 GeV. A cut of $E_{\gamma_2} < 5$ GeV has been applied to the phase space of the semi-collinear photon

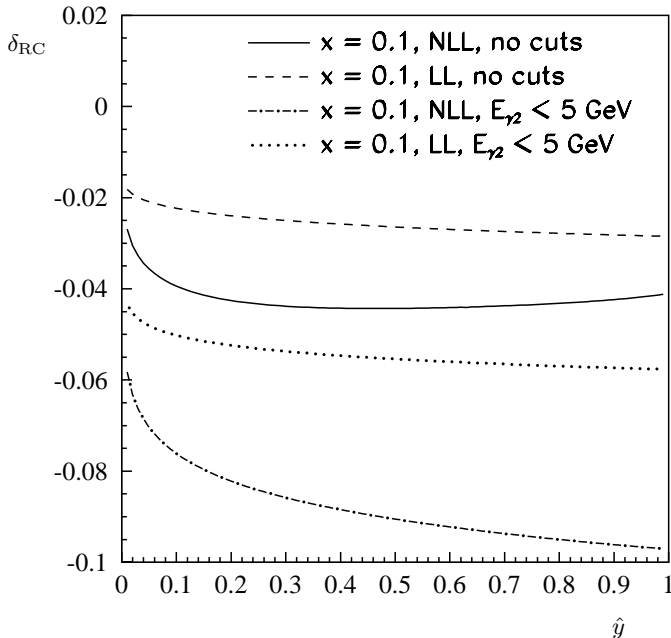


Fig. 4. Comparison of the cut dependence of the radiative corrections at $\hat{x} = 0.1$ for a tagged photon energy of 5 GeV. A cut of $E_{\gamma_2} < 5$ GeV has been applied to the phase space of the semi-collinear photon

Finally, Fig. 6 shows the dependence of the next-to-leading logarithmic corrections on the ratio R (see 27), again for $\hat{x} = 0.1$ and $\hat{x} = 10^{-4}$ and for a tagged energy of $E_{PD} = 5$ GeV. As one would expect, one sees that only for large \hat{y} there is a visible difference between the corrections calculated for (assumed constant) $R = 0$ and $R = 0.3$ of the order of a permille. In the case of the purely leading logarithmic corrections the change would be much less than the order of the line width, so we omitted the corresponding lines. For this reason, a poorly known $R(x, Q^2)$ as input to the calculation of the QED corrections will not have any significant effect on the extraction [4] of R from the measured tagged photon cross section. Increasing the value of R up to, say, $R = 1$ for the smaller value of \hat{x} would simply increase the difference with respect to the curve for $R = 0$ but not lead to a qualitative change of our conclusions.

5 Summary

The Σ method for the determination of the kinematic variables in deep inelastic scattering has been reviewed in some detail from a theoretical point of view. We derived the relevant kinematics for the calculation of the hard photon emission contributions of the QED corrections to deep inelastic scattering for the HERA collider. As an application, we extended the formalism to radiative DIS events with a hard photon tagged in the forward photon detectors of the H1 and ZEUS experiments. We

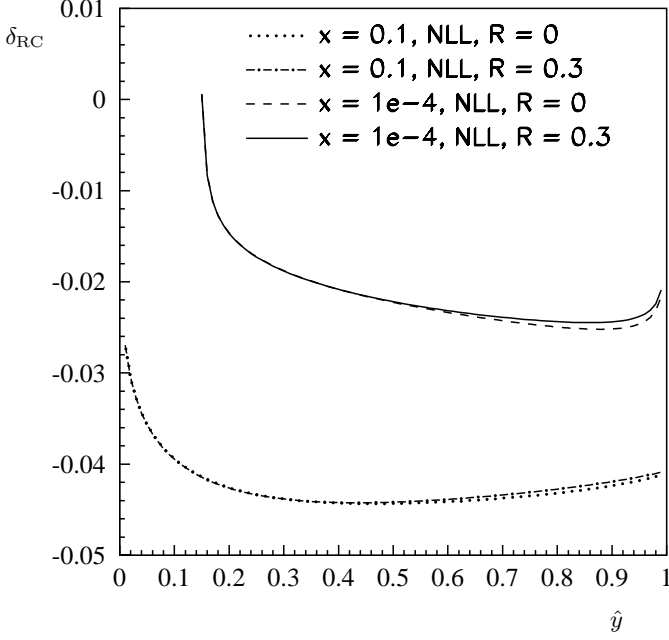


Fig. 6. Comparison of the R dependence of the NLL corrections at $\hat{x} = 0.1$ and $\hat{x} = 10^{-4}$ for a tagged photon energy of 5 GeV. No cut has been applied to the phase space of the semi-collinear photon

have adapted the calculations [7–9] of the radiative corrections to these DIS events with a tagged photon for the Σ method determination of kinematic variables. It turned out that for a calorimetric measurement of the final state lepton the leading-logarithmic corrections are suppressed and thus quite small (of the order of 5%), which is an intrinsic feature of the Σ method. However, the typical size of the unsuppressed next-to-leading logarithmic contributions is of the same order of magnitude. However, for a bare event selection there are also significant contributions to the corrections already at the leading logarithmic level.

The smallness of the leading QED corrections for the Σ method suggests that the corrections are well under control, so that neglected higher order corrections will not play a significant rôle. It is also encouraging that the dependence of the corrections on the poorly known longitudinal structure function F_L (and thus R) is very small.

It is a great pleasure to thank A.B. Arbuzov, M. Fleischer and H. Spiesberger for a critical reading of the manuscript and many useful suggestions.

A Kinematic limit of hard photon emission

This appendix is devoted to a discussion of the phase space limit for the emission of a hard photon in radiative DIS in the case of the Σ method. As we shall refer exclusively

to the Σ method, and to avoid cumbersome notation, we drop the index Σ from all kinematic variables.

In the parameterization of the photon phase space following from (4), the invariant mass of the hadronic system (18) is

$$\begin{aligned} W^2 &= M^2 + yS \left(1 - \kappa - \frac{x}{1 - \kappa} \right) - 2x_\gamma E_e^2 (1 - \cos \vartheta) \\ &\quad + 2x_\gamma E_e E_e' (1 - \cos \vartheta') \\ &= M^2 + yS [1 - \kappa - x] \\ &\quad - 4E_e^2 \frac{1 - \cos \vartheta}{1 + \cos \vartheta} \kappa [1 - (1 - \kappa)(1 - y)] \\ &\quad - 4\kappa E_e \sqrt{xy(1 - y)} S \sqrt{\frac{1 - \cos \vartheta}{1 + \cos \vartheta}} \cos \varphi, \end{aligned} \quad (44)$$

where we heavily used the relations (12)–(15) and

$$\kappa = x_\gamma \frac{1 + \cos \vartheta}{2}. \quad (45)$$

With the help of the following abbreviations,

$$\begin{aligned} \mu &= 1 - x - \frac{\bar{M}^2 - M^2}{yS} \equiv 1 - x - \frac{\bar{\Delta}_m}{y}, \\ \lambda &= \sqrt{\frac{E_e}{E_p} \frac{1 - \cos \vartheta}{1 + \cos \vartheta}} \\ \nu &= \sqrt{4xy(1 - y)} \cos \varphi, \end{aligned} \quad (46)$$

which satisfy the constraints

$$0 \leq \mu < 1, \quad 0 \leq \lambda < \infty, \quad |\nu| < 1, \quad (47)$$

the inequality $W^2 \geq \bar{M}^2$ can be brought into a simpler form:

$$y\mu - [y(1 + \lambda^2) + \lambda\nu] \kappa - \lambda^2(1 - y)\kappa^2 \geq 0. \quad (48)$$

Obviously the physical range is $0 \leq \kappa \leq \kappa_0$, with

$$\begin{aligned} \kappa_0 &= -\frac{y(1 + \lambda^2) + \lambda\nu}{2\lambda^2(1 - y)} \\ &\quad + \frac{\sqrt{[y(1 + \lambda^2) + \lambda\nu]^2 + 4y(1 - y)\mu\lambda^2}}{2\lambda^2(1 - y)}. \end{aligned} \quad (49)$$

Direct inspection of (48) shows that for $y \rightarrow 1$, κ_0 approaches the value

$$\tilde{\kappa}_0 \equiv \kappa_0(y = 1) = \frac{1 - x - \bar{\Delta}_m}{1 + \lambda^2} < 1. \quad (50)$$

Note that the choice of ϑ and φ for the parameterization of the photon phase space is not well suited for analytic or semi-analytic calculations, as the treatment of the separation between the phase space regions *ii*) and *iii*) in Sect. 3 is rather cumbersome.

B Parameterization of the hard photon phase space

Instead of using the parameterization (4) for the phase space of the hard photon, it is often convenient to trade the azimuthal angle φ in favor of the angle ϑ' between the photon and the final state lepton. Introducing the variables τ_1, τ_2 ,

$$\tau_1 := \frac{1 - \cos \vartheta'}{2}, \quad (51)$$

$$\tau_2 := \frac{1 - \cos \vartheta''}{2} = \frac{1 - \cos \theta \cos \vartheta' - \sin \theta \sin \vartheta' \cos \varphi}{2},$$

the integration over the photon solid angle becomes

$$\int d\Omega_\gamma \equiv \int d(\cos \vartheta) d\varphi = \int \mathcal{J}(\tau_1, \tau_2) \Theta(\mathcal{D}) d\tau_1 d\tau_2, \quad (52)$$

with the Jacobian

$$\mathcal{J}(\tau_1, \tau_2) = \frac{8}{|\sin \theta \sin \vartheta \sin \varphi|} =: \frac{4}{\sqrt{\mathcal{D}}},$$

where

$$\mathcal{D} = -4\tau_1\tau_2 - (\tau^2 + \tau_1^2 + \tau_2^2 - 2\tau\tau_1 - 2\tau\tau_2 - 2\tau_1\tau_2), \quad (53)$$

$$\tau := \frac{1 - \cos \theta}{2} = \frac{xy\varepsilon}{(1 - \kappa)^2(1 - y) + xy\varepsilon}, \quad (54)$$

$$\varepsilon := \frac{E_p}{E_e}.$$

A factor of 2 has been taken into account in the Jacobian for the two-fold ambiguity in the azimuthal angle φ . Note that $0 \leq \kappa < 1$ implies

$$\tau \geq \tau^{(0)}(x, y) \equiv \frac{xy\varepsilon}{1 - y + xy\varepsilon}. \quad (55)$$

The range of integration for the variables $\tau_{1,2}$ for a given photon energy $x_\gamma E_e$ follows from the argument of the step function $\Theta(\mathcal{D})$. It is trivially obtained if τ depends only on the kinematic variables x, y but not on the photon phase space variables, as is the case for a purely leptonic measurement of the kinematic variables [9], but it is more involved for the Σ method and will therefore be discussed below.

As the relevant variables for the parameterization of the phase space of the photon we choose τ_1, τ_2 , and x_γ . Due to (54), τ is related to x_γ , as $\kappa = x_\gamma(1 - \tau_1)$. Therefore, it appears to be reasonable to take τ_1 as the outermost integration and to determine the range of integration for the other two variables for each value of τ_1 , $0 < \tau_1 < 1$.

Obviously, the range where the argument \mathcal{D} (53) of the Θ function above is positive is given by the interior of an ellipse as shown in Fig. 7. The ellipse touches the τ - and τ_2 -axes at the value of τ_1 , and the lines $\tau = 1$ and $\tau_2 = 1$ at the value of $(1 - \tau_1)$.

The explicit form of the upper and lower boundaries of the ellipse are

$$\tau_2^\pm(\tau_1, \tau) = \tau_1(1 - \tau) + \tau(1 - \tau_1) \pm 2\sqrt{\tau_1(1 - \tau)\tau(1 - \tau_1)}. \quad (56)$$

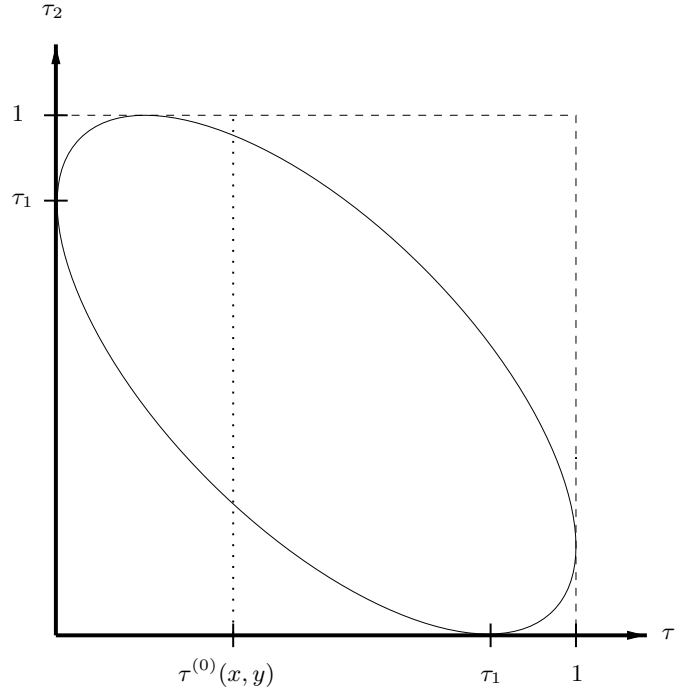


Fig. 7. Schematic view of the kinematic range for the integration over the angles τ and τ_2 for fixed τ_1 . The allowed range from the change of variables (51) alone is given by the interior of the ellipse. In addition, for given x, y , the region left to the dotted line is unphysical, as $\tau \geq \tau^{(0)}(x, y)$ from (55)

On the other hand, remembering that for given x, y there is a lower limit (55) on τ , we see that the part of this ellipse left to the dotted line is certainly unphysical.

Yet we have not made use of a lower limit on the hadronic mass that is due to the inelastic threshold or to a lower cut on the invariant hadronic mass. To this end, we express the hadronic mass (44) in terms of the $\tau_{1,2}$:

$$\begin{aligned} W^2 &= M^2 + yS \left(1 - \kappa - \frac{x}{1 - \kappa} \right) \\ &\quad - 4x_\gamma E_e^2 \tau_1 + 4x_\gamma E_e E_e' \tau_2 \\ &= M^2 + yS \left[1 - \kappa - \frac{x}{1 - \kappa} \right] - \frac{S}{\varepsilon} \frac{\tau_1}{1 - \tau_1} \kappa \\ &\quad + S \frac{\tau_2}{1 - \tau_1} \left[\frac{(1 - \kappa)(1 - y)}{\varepsilon} + \frac{xy}{1 - \kappa} \right] \kappa. \end{aligned} \quad (57)$$

Requiring $W^2 \geq \bar{M}^2$ leads to the inequality

$$W^2 - \bar{M}^2 = \frac{S}{(1 - \kappa)(1 - \tau_1)} [A\kappa^3 + B\kappa^2 + C\kappa + D] \geq 0$$

where

$$\begin{aligned} A &= \frac{(1 - y)\tau_2}{\varepsilon} \\ B &= (1 - \tau_1)y + \frac{\tau_1 - 2(1 - y)\tau_2}{\varepsilon} \\ C &= xy\tau_2 - 2y(1 - \tau_1) + (1 - \tau_1)\bar{\Delta}_m \\ &\quad + \frac{(1 - y)\tau_2 - \tau_1}{\varepsilon} \end{aligned} \quad (58)$$

$$D = (1 - \tau_1) [(1 - x)y - \bar{\Delta}_m] .$$

Since $A \geq 0$, $D > 0$, the cubic equation $A\kappa^3 + B\kappa^2 + C\kappa + D = 0$ will have either one or three real solutions: always a negative one which is obviously unphysical, and two positive or complex conjugate ones.

In case there are three real solutions, only the smaller one of the two positive solutions may be physical. This may be seen by studying the limit $\tau_1 \rightarrow 1$, where κ has to go to 0 for any finite photon energy x_γ .

For small values of τ_2 , i.e., radiation collinear to the outgoing lepton, one always has three real solutions. This is easily verified by direct inspection of (58) for $A \rightarrow 0$: the negative solution goes to $-\infty$ essentially as $-B/A$, and the resulting quadratic equation in the limit $\tau_2 = 0$ always has a positive discriminant.

In the remaining cases when there is only one real (and negative) solution, the effective upper limit on κ may be indirectly obtained from (54) and the maximum allowed value for τ^+ as a function of $\tau_{1,2}$, similarly to (56),

$$\kappa \leq \bar{\kappa}(\tau_1, \tau_2) \equiv 1 - \sqrt{\frac{1 - \tau^+}{\tau^+} \frac{\tau^{(0)}}{1 - \tau^{(0)}}}, \quad (59)$$

which is entirely of geometric origin.

Let us now compare the above limits that were derived from the lower limit (or a cut) on the hadronic mass with the kinematic limits for collinear photon radiation, as given in [12]. The case of collinear initial state radiation (ISR) is recovered by setting $\tau_1 \rightarrow 0$, so that $\kappa \rightarrow x_\gamma$, $\tau_2 E'_e \rightarrow xyE_p/(1 - x_\gamma)$, and from (57) one immediately obtains

$$x_\gamma \leq 1 - x - \frac{\bar{\Delta}_m}{y}. \quad (60)$$

This is consistent with the limit on $z (= 1 - x_\gamma)$ given in [12] up to terms of order $\mathcal{O}(\bar{\Delta}_m)$, as these authors did not consider neither the inelastic threshold nor a cut on the hadronic mass.

Collinear final state radiation (FSR) corresponds to taking the limit $\tau_2 \rightarrow 0$, $\tau_1 \rightarrow \tau = xy\varepsilon/\{[1 - x_\gamma(1 - \tau)]^2 \times (1 - y) + xy\varepsilon\}$, with τ being implicitly defined. However, in order to be able to compare our limit with the one given in [12], we shall think of the collinear photon as taking away the fraction $(1 - \zeta)$ of the outgoing lepton-photon system, while the lepton retains the fraction ζ . Hence, we have $k = [(1 - \zeta)/\zeta]p'$, and we may write

$$P \cdot k = \frac{1 - \zeta}{\zeta} P \cdot p' \implies \frac{\kappa}{1 - \kappa} \frac{\zeta}{1 - \zeta} = 1 - y, \\ 1 - \kappa = \frac{\zeta}{1 - y(1 - \zeta)}, \quad (61)$$

and thus

$$p \cdot k = \frac{1 - \zeta}{\zeta} p \cdot p' = \frac{xy}{1 - \kappa} \frac{1 - \zeta}{\zeta} \cdot \frac{1}{2} S \\ = \frac{xy[1 - y(1 - \zeta)](1 - \zeta)}{\zeta^2} \cdot \frac{1}{2} S. \quad (62)$$

Inserting these relations into (18) we obtain

$$W^2 \Big|_{\text{FSR}} = M^2 + \frac{\zeta^3 - x[1 - y(1 - \zeta)]^2}{\zeta^2[1 - y(1 - \zeta)]} yS \geq \bar{M}^2. \quad (63)$$

This inequality leads to a lower limit ζ_0 , $0 < \zeta_0 < 1$, that is the single real solution of a cubic equation, $W^2(\zeta_0) = \bar{M}^2$. The kinematic limit that follows from (63) is consistent with the limit for FSR given in [12], again up to terms of order $\mathcal{O}(\bar{\Delta}_m)$ that have been neglected in their work.

Finally, we should mention that the above considerations directly apply only to the case of conventional deep inelastic scattering with a single radiated photon. However, the case of DIS with a tagged collinear photon and a hard non-collinear second photon is easily recovered, provided we perform the simultaneous substitutions

$$E_e \rightarrow zE_e, \quad S \rightarrow zS, \quad x_\gamma \rightarrow \frac{x_2}{z}, \quad \kappa \rightarrow \frac{\kappa}{z}, \\ \varepsilon \rightarrow \frac{\varepsilon}{z}, \quad \text{and} \quad \bar{\Delta}_m \rightarrow \frac{\bar{\Delta}_m}{z} \quad (64)$$

in the expressions given above.

References

1. M.W. Krasny, W. Płaczek, H. Spiesberger, Z. Phys. C **53**, 687 (1992)
2. H1 Collaboration (T. Ahmed, et al.), Z. Phys. C **66**, 529 (1995)
3. ZEUS Collaboration (M. Derrick, et al.), Z. Phys. C **69**, 607 (1996)
4. L. Favart, M. Gruwé, P. Marage, Z. Zhang, Z. Phys. C **72**, 425 (1996)
5. M. Klein (H1 collaboration), talk no. 404 given at the ICHEP98 conference, (Vancouver, Canada, July 1998), and contributed paper no. 535
6. G. Wolf, DESY 97-047, 1997, hep-ex/9704006 (unpublished)
7. H. Anlauf, A.B. Arbuzov, E.A. Kuraev, N.P. Merenkov, Phys. Rev. D **59**, 014003 (1999)
8. H. Anlauf, A.B. Arbuzov, E.A. Kuraev, N.P. Merenkov, JETP Lett. **66**, 391 (1997); *ibid.* **67**, 305(E) (1998)
9. H. Anlauf, A.B. Arbuzov, E.A. Kuraev, N.P. Merenkov, JHEP **10**, 013 (1998)
10. U. Bassler, G. Bernardi, Nucl. Instrum. Meth. A **361**, 197 (1995)
11. H. Anlauf, H.D. Dahmen, P. Manakos, T. Mannel, T. Ohl, Comp. Phys. Comm. **70**, 97 (1992)
12. A.B. Arbuzov, D. Bardin, J. Blümlein, L. Kalinovskaya, T. Riemann, Comput. Phys. Commun. **94**, 128 (1996)
13. D. Bardin, J. Blümlein, P. Christova, L. Kalinovskaya, in *Proceedings of the Workshop on Future Physics at HERA*, edited by G. Ingelman, A. De Roeck, R. Klanner (DESY, Hamburg, 1996), p. 13
14. D. Bardin, L. Kalinovskaya, T. Riemann, Z. Phys. C **76**, 487 (1997)
15. W. Beenakker, F.A. Berends, S.C. van der Marck, Nucl. Phys. B **349**, 323 (1991)
16. T. Kinoshita, J. Math. Phys. (N.Y.) **3**, 650 (1962); T.D. Lee and M. Nauenberg, Phys. Rev. **133**, 1549 (1964)
17. H. Abramowicz, A. Levy, DESY 97-251, 1997, hep-ph/9712415 (unpublished)